Bull Earthquake Eng (2013) 11:241–254
DOI 10.1007/s10518-012-9385-4

ORIGINAL RESEARCH PAPER

A note on the strong ground motion recorded during the Mw 6.8 earthquake in Myanmar on 24 March 2011

Teraphan Ornthammarath

Received: 3 August 2012 / Accepted: 17 September 2012 / Published online: 26 September 2012

Abstract This study aims to investigate a Mw 6.8 earthquake that occurred in Myanmar on 24 March 2011. The epicenter of this earthquake struck very close to the Tarlay town which is located near the border of Myanmar, Lao People's Democratic Republic (PDR), and Thailand. In addition, this shallow left-lateral strike-slip earthquake occurred on Nam Ma fault which is previously identified as an active fault. Based on instrumental earthquake catalogue, Nam Ma fault did not produce any earthquake greater than magnitude 6 for at least 100 years. So the 24 March 2011 earthquake is essentially filling the gap of relatively short instrumental earthquake catalogue in this region. The strong ground motion from this event has been recorded in Thailand with the highest peak ground acceleration (PGA) of 0.20 g at 28 km distance at Mae Sai town. Comparison between observed strong motion and global empirical equation had been provided. Over the distance range for which the model is applicable, they are in fair agreement. On the other hand, at long distance, the large positive and negative residuals suggest that a change in slope in the attenuation is not reflected in these relations. Lastly a seismological aspect of strong ground motion at Mae Sai had been given.

Keywords Myanmar earthquake · Strong ground motion · Nam Ma fault

1 Introduction

On 24 March 2011, a strong earthquake of Mw 6.8 with shallow focal depths around 10 km struck northeast Myanmar very close to Tarlay and Mong Hpayak cities at 13.55 GMT. Since the epicenter of this earthquake located near the border of Myanmar, Lao PDR, and Thailand (commonly known as Golden triangle area), this earthquake was widely felt in most

T. Ornthammarath (✉)
Regional Integrated Multi-Hazard Early Warning System (RIMES), Pathumthani, Thailand
e-mail: teraphan@rimes.int

T. Ornthammarath
Asian Institute of Technology, Pathumthani, Thailand

parts of Myanmar, northern part of Thailand, northwestern part of Lao PDR, southern part of Yunnan, China as well as people in the high-rise buildings in Bangkok and Hanoi. Soon after, the extensive damage inside Myanmar start to emerge with reports of 70 casualties or more with many injured victims, total structural collapse, landslide, and one collapsed bridge corresponding to Modified Mercalli Intensity (MMI) about VIII in Tarlay township. Despite severe damage to infrastructure and residential houses in Myanmar, the observed damage in Mae Sai district, which is Thai border city locating around 30 km from the epicenter, are relatively less intense with one casualty from collapsed wall, cracking inside buildings, liquefaction, local lateral spreading, toppled top part of the eleventh century stupa; however, there is no report of building collapse (MMI VI; Ruangrassamee et al. 2012).

The strong ground motion of this event had been recorded by 20 digital accelerometers operated by Thai Metrological Department (TMD); however, only four stations were located within 200 km from the mainshock, with one being within 28 km of the originated fault. The largest horizontal PGA from this event is 0.20 g, which is the highest ground motion ever recorded in Thailand. In addition, Thailand seismic network has just been significantly improved following devastating magnitude of 9.2 Sumatra earthquake in 2004. This article provides an overview of the local seismotectonic settings relating to 24 March 2011 event, characteristic of observed strong motion with available ground motion prediction equations (GMPEs), and some interesting results observed from strong ground motion recorded at Mae Sai station.

2 Regional seismotectonic setting and 24 March 2011 earthquake

On a continental scale, the 24 March 2011 event clearly reminds us the stress in Sundaland block which is built up by ongoing collision process between two tectonic plates, the Indian and the Eurasian plates. Currently the Indian plate is still pushing northward at a rate of 45 mm/year inducing an anti-clockwise rotation of the Indian plate (Bilham 2004), and the Sundaland block moves eastward with a clockwise rotation. One common pattern of active faults in golden triangle region is left-lateral NE-SW to ENE-SWS striking faults to accommodate two major right lateral strike-slip Red River fault in Vietnam and Sagaing fault in Myanmar. This pattern is characterized by bookshelf types of tectonic, which means that the golden triangle area is described as a stack of rotated blocks creating numbers of secondary faults between these two major faults. These secondary faults, e.g. Nam Ma, Menglian, Mengxing, Dien Bien Phu, and Mae Chan faults (e.g. Lacassin et al. 1998; Fenton et al. 2003; Uttamo et al. 2003; Shen et al. 2005), which have been less studied than those two main faults, are proved to be a threat to any infrastructures in this region as well.

The Nam Ma fault, a NE-SW trending strike-slip fault, is believed to generate the 24 March 2011 event. This fault originates in southern China, extends into northwestern Laos and propagates in northeastern Myanmar. It continues to the southwest and terminates near the Salween River. The total legnth of this fault is approximately around 150 km. From epicentral location of 24 March 2011 event, only western segment of Nam Ma fault is responsbile for this event. Lacassin et al. (1998) used the mosaic of SPOT multispectral images to identify the geomorphic evidence of residual right lateral bends that remain after restoring the left-lateral offset around 12 km on the Mekong River, Fig. 1. The estimated slip rate of this fault based on the relationship of river offsets and ages of rocks is in between 0.6 and 2.4 mm/yr, which is comparable to the slip rates of other secondary faults in this area (Lacassin et al. 1998). Based on Thailand earthquake catalogue and its surrounding region from 1912 to 2011 (Ornthammarath et al. 2011), Nam Ma fault did not produce any earthquake greater

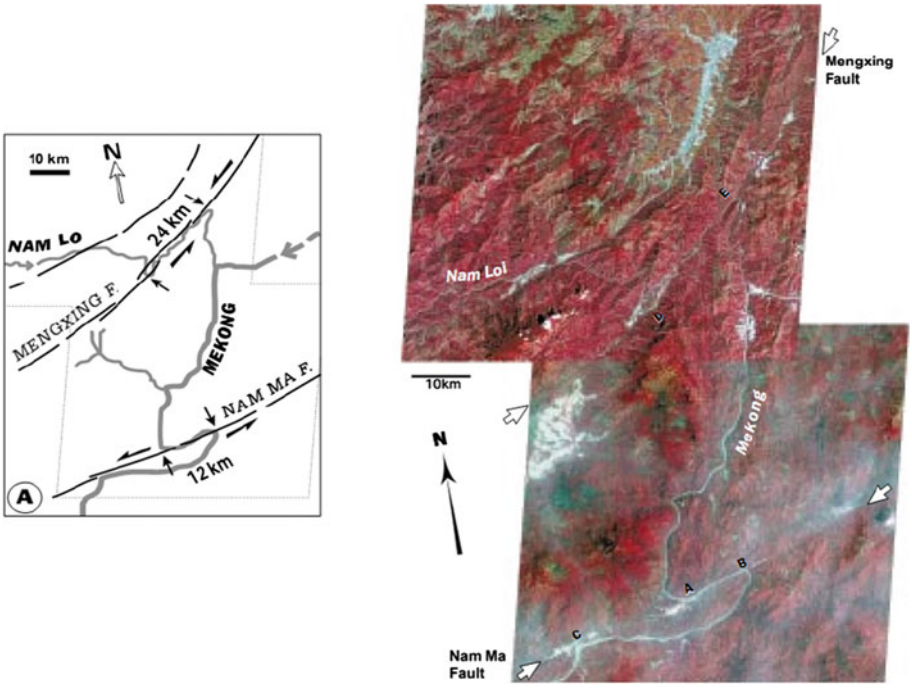

Fig. 1 Location of Nam Ma fault and its geomorphic evidence of displacement residual around 12 km on the Mekong River, (Lacassin et al. 1998)

than magnitude 6 for at least 100 years, Fig. 2. So the 24 March 2011 earthquake is essentially filling the gap of relatively short instrumental earthquake catalogue in this region. Magnitude and epicenter of the earthquake are defined by various institutions as given in Table 1. In addition, all previous probabilistic seismic hazard assessments (PSHA) in the area have foreseen moderate hazard level with PGA at 475-year return period larger than 0.20 g (Giardini et al. 1999; Palasri and Ruangrassamee 2010; Ornthammarath et al. 2011).

Later on, the first motion focal mechanism of this tremor had been determined with an almost pure left-lateral strike slip mechanism, confirming previous seismotectonic information. Moreover, the modeled focal mechanism by Global CMT, Table 2, which is based on long period waveform solution, suggests similar fault orientations with more eastwardly location, Fig. 2. Owning to determined location uncertainties of NEIC and Global CMT (Ekstrom, G., personal communication, 2011), this pattern might suggest that the earthquake begin at the southwestern part and ruptured toward northeast, where Tarlay and Mong Hpayak cities are located resulting in high casualities in these two towns. Moreover, there were reports of several aftershocks following mainshock for several months as reported by local people and TMD. The biggest aftershock of M_W 5.7 shook this region two hours after main event having epicenter near mainshock with similar focal mechanism.

From 24-hour aftershock distribution data from TMD the rupture length of this event should not be greater than a couple of 10 km. It is later confirmed by local field investigation at epicentral region that the observed surface rupture length is around 32 km with offset from 0.30 to 1.25 m (Soe Thura Tun, personal communication, 2011) in close agreement with Wells and Coppersmith (1994)'s magnitude and rupture length relationship that the average

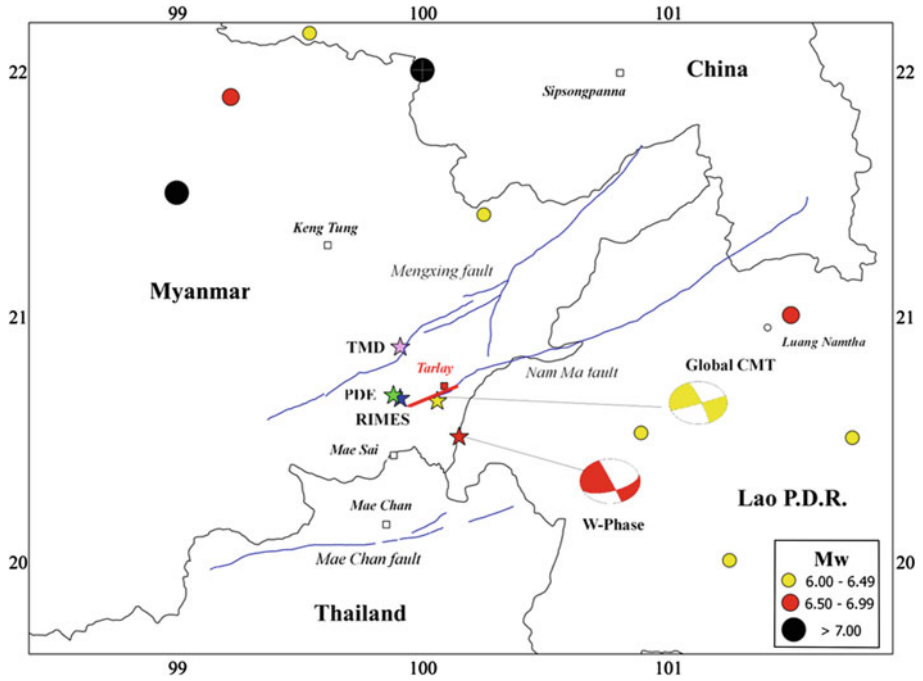

Fig. 2 Map of the Golden Triangle area with instrumental seismicity for earthquake magnitude greater than 6.0 from 1912 to 2011. The *blue lines* represent major active faults in this region. The epicentral and centroid locations of Tarlay earthquake determined by different earthquake observatories have also been shown, PDE (Preliminary Determination of Epicenters); TMD (Thai Metrological Department); RIMES (Regional Integrated Multi-Hazard Early Warning System). The *red line* indicates rupture area of 24 March 2011 event

Table 1 Characteristics of 24 March 2011 13.55 (GMT) Tarlay Earthquake

Source	Coordinates		Magnitude	Depth (km)
	N	E		
RIMES[a]	20.68	99.83	6.7 (M_W(MB))	10
TMD[b]	20.87	99.91	6.7 (M_L)	10
USGS[c]	20.69	99.82	6.8 (M_W)	8
Global CMT[d]	20.62	100.02	6.8 (M_W)	13.2

[a] Regional Integrated Multi-Hazard Early Warning System (www.rimes.int)
[b] Thai Metrological Department (www.seismology.tmd.go.th)
[c] NEIC PDE catalog (http://earthquake.usgs.gov/earthquakes/eqarchives/epic/)
[d] Global CMT (http://www.globalcmt.org)

Table 2 Information on the mainshock nodal planes and the moment magnitude (M_W) estimated by various institutions: GCMT, USGS

Source	Nodal Plane 1			Nodal Plane 2		
	Strike	Dip	Rake	Strike	Dip	Rake
USGS	250	86	−2	340	88	−176
Global CMT	70	85	11	339	79	175

surface rupture length is about 30 km. Knopoff (1958) obtained the stress drop from a shallow strike-slip motion of rectangular fault of length L and width w by

$$\Delta\sigma = \frac{2M_0}{\pi w^2 L} \tag{1}$$

where M_0 is seismic moment. The stress drop of Tarlay earthquake should be from 27 to 16 bar by assuming from 13 to 15 km rupture width and from 32 to 40 km rupture length. The assumed fault rupture areas have found to be in good agreement with that of Wells and Coppersmith (1994). Tarlay earthquake's stress drop is then approximately consistent with that of interplate region (Stein and Wysession 2003). Kagawa et al. (2004) found that the buried rupture tend to produce higher stress drops than that of surface rupture. However, Radiguet et al. (2009) found small differences between ground motion from buried and surface rupturing events, and conclude that the difference observed by Kagawa et al. (2004) might be related to sample size effects and site response biases.

3 Recorded strong ground motion

The strong ground motion of the Tarlay earthquake were recorded by 20 free-field digital strong motion instruments of TMD network; however, only four of these instruments are located at distance less than 200 km from originated fault, Table 3. The closest distance from the instruments to the surface projection of the fault are taken from the approximated fault location described in section 2. Currently, there are three different kinds of triaxial digital accelerometers that have been deployed by TMD, but only strong motion data recorded by PA-23 model of Geotech with 24-bit A/D converter have been acquired from this event.

Based on available borehole profiles from nearby seismic stations, of those 20 stations, 14 sites can be classified as soil type D, and four sites are classified as soil type C. Only Bangkok seismic station is evaluated as soil type E since the city is situated on a large and extremely flat plain. The lower central plain consists of a broad deep basin filled with alluvial and deltaic sediments with depth of bedrock surface around 550 m. The length from north to south of the plain is about 250 km and the average width is approximately 200 km, (AIT 1980).

All records have been obtained and performed the standard zero–order correction. Subsequently, the acceleration records have been integrated to obtain velocity and displacement time histories. If records have been affected by baseline distortion, the baseline correction technique proposed by Rupakhety et al. (2010) and Sigurdsson et al. (2011) have been performed. All reported ground motions are a direction-independent average horizontal ground

Table 3 Strong motion stations within 200 km that recorded the mainshock with their parameters

Station	Location		NEHRP site class	R_{jb} (km)	R_{epi} (km)	Source-to-Site Azimuth (degree)	Ground motions			
	Lat (N)	Long (E)					PHA (g)	PHV (cm/s)	PVA (g)	D5–95 (s)
MAES	20.428	99.886	D	28	28	169	0.20	12.7	0.11	13.8, 14.4
CRAI	20.229	100.373	C	64	75	132	0.07	5.1	0.03	16.1, 14.2
PAYA	19.360	99.869	D	146	147	178	0.015	1.9	0.009	30.0, 33.9
NAN	19.283	100.912	C	190	191	143	0.005	2.1	0.004	44.5, 27.2

motion (GMrotl50). Peak horizontal acceleration (PHA), peak horizontal velocity, and peak vertical acceleration (PVA) are shown in Table 3 along with significant duration (D 5-95).

Comparison of observed ground motion from Mw 6.8 Tarlay earthquake to Boore and Atkinson (2008), BA08, which is developed as part of Next Generation Attenuation (NGA) project and Sadigh et al. (1997) versus distance are shown in Fig. 3 for PHA and Spectral acceleration (SA) at 0.2 and 1.0 s. Since, in this region, there is a very limited number of available strong motion records, some existing GMPEs developed for other similar seismotectonic setting is assumed to be adequately represent ground motion scaling in this region. In addition, both Sadigh et al. (1997) and BA08 relations have been adopted in recent probabilistic seismic hazard analysis for Thailand (Ornthammarath et al. 2011; Palasri and Ruangrassamee 2010). The selected V_{S30} for soil condition between C/D NEHRP site class in NGA equations is 360 m/s has been chosen for BA08. For Sadigh et al. (1997) relation, the deep soil site condition has been chosen to compare with observed strong motion data. Median (μ) and $\pm$ one standard deviation (σ) are shown for both equations. It could be quickly noticed that the soil amplification in Bangkok is much larger than that of similar distance for about 2 to 3 times for all considered structural periods.

In addition, to more accurately evaluate the performance of the GMPEs relative to data, the computed residual has been performed to understand the average characteristic of the Tarlay earthquake ground motion to that of global equations. The residual for each data point comparing to that estimated by GMPEs are defined as:

$$R_{\mathrm{i}} = \ln (SA_{\mathrm{i}})_{rec} - \ln (SA_{\mathrm{i}})_{GMPE} \tag{2}$$

where $(SA_{\mathrm{i}})_{rec}$ = values of SA from recording i and$(SA_{\mathrm{i}})_{GMPE}$ = median value of SA from GMPE. The evaluated strong motion parameters are PGA and SA at 0.2 and 1.0 s for both BA08 and Sadigh et al. (1997) equations, Fig. 4.

Some principal trends illustrated by Figs. 3 and 4 are as follows:

- For BA08 GMPE, the residual for PHA and SA at 0.2 s generally exhibit no significant bias over the applicable distance range from 0 to 200 km; however, large positive residuals at larger distance indicate underestimation of GMPE comparing to that of recorded ground motion. In contrast to Sadigh et al. (1997), the residual for PHS and SA at 0.2 s show negative residual at large distance indicating faster attenuation in the recorded data than that in the model. In addition, it should be noted that the large residuals beyond 200 km are to be expected since most GMPEs are derived to estimate ground motions up to 200 km.
- For SA at 1.0 s, residuals of both GMPEs have a negative value with distance which reveals that recorded SA at 1.0 s of Tarlay earthquake is overestimated by both equations.
- At Mae Sai station, both observed PHA and SA at 0.2 s are underestimated by both relations; however, they are inside the median plus one standard deviation. In contrast, the observed SA at 1.0 s is below medians for both equations.

4 Strong Ground Motion at Mae Sai station

From 24 March 2011 event, the nearest accelerograph station is in Mae Sai district, located 28-km distance from fault rupture. Geologically, Mae Sai basin was developed as a pull-apart basin between the sinistral movement of the Nam Ma and Mae Chan faults with deep deposited sediment (Uttamo et al. 2003). Shear-wave velocities obtained by an array-micro-

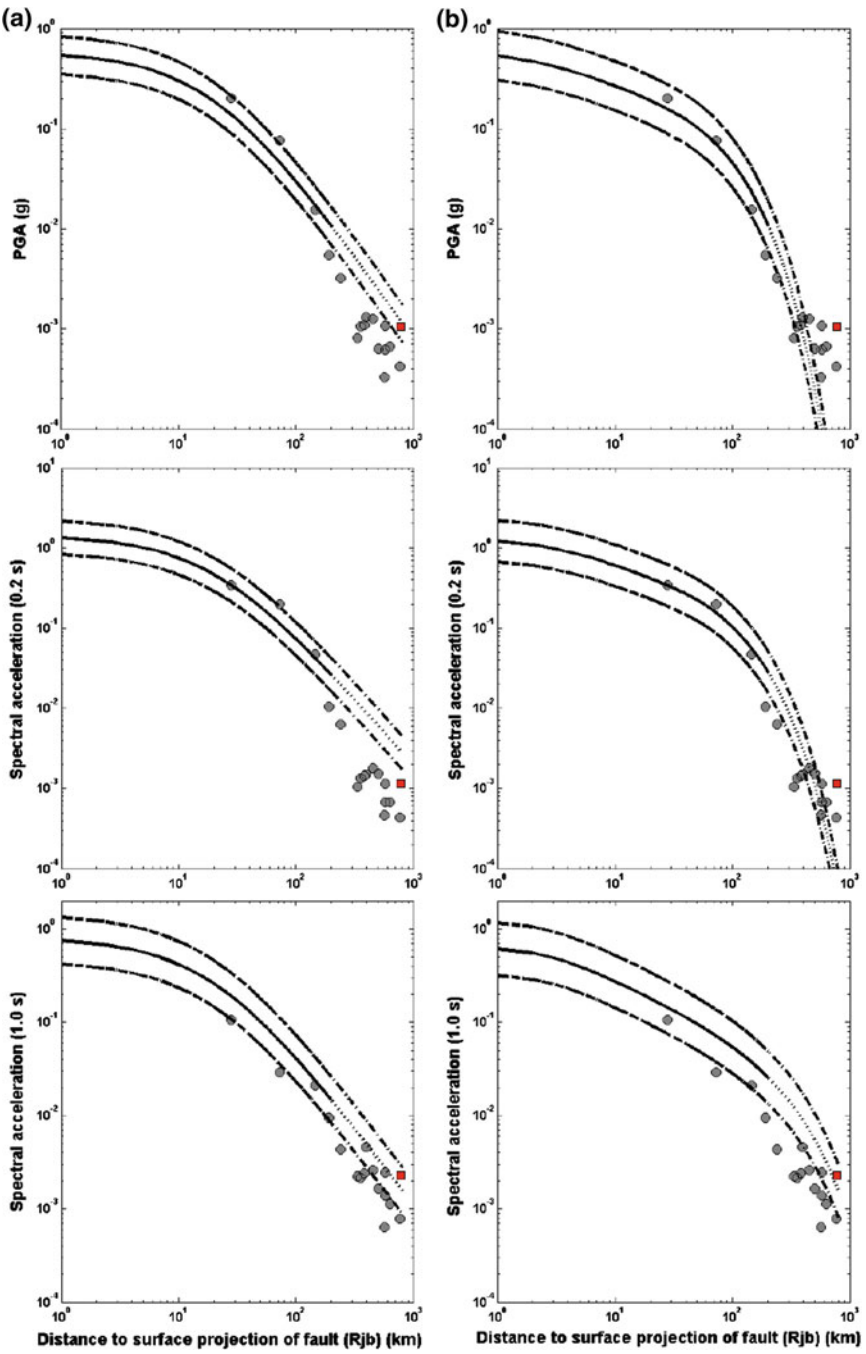

Fig. 3 Comparison of PGA and SA at 0.2 and 1.0 s from Tarlay earthquake ground motions to median and median ± one standard deviation of **a** Sadigh et al. (1997) and **b** BA 08. Observed ground motion is in *gray circles* while Bangkok ground motion is in *red square* to show the effect of soil amplification at the same distance. Note that different line styles are being used for estimated ground motion parameters at distance larger than 200 km

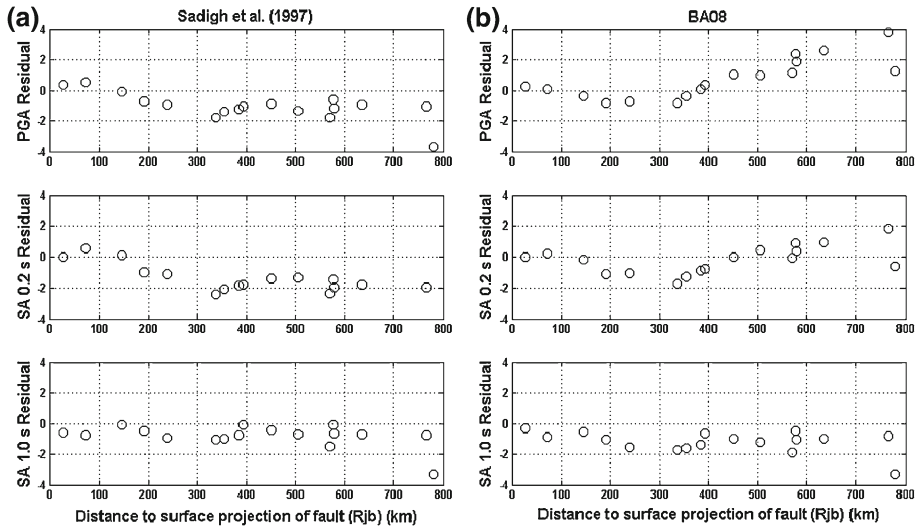

Fig. 4 Residual of ground motion parameters from recorded ground motions relative to predictions of **a** Sadigh et al. (1997) and **b** BA08 GMPE

tremor analysis at the site by Poovarodom and Pitakwong (2010) are relatively low, with an average velocity over the upper 30 m of 335 m/s, corresponding to NEHRP site category D (180 m/s $< V_{S(30)} <$ 360 m/s). At this station, the observed PGA in NS, EW, and UD reach 0.19, 0.20, and 0.11 g, respectively. Although the horizontal PGA is relatively high, which might be due to local soil amplification, but the observed damage inside Mae Sai area is rather low comparing to that inside Myanmar. Based on probabilistic relationship between MMI and PGA developed by Worden et al. (2012), the MMI around VII could be expected. Possible answers to this question could be related to location of Mae Sai which is rather away from originated fault and the observed horizontal peak ground velocity (PGV) is just 15 cm/s, and PGV is usually correlated well with observed damage than that of PGA (e.g., Wald et al. 1999; Akkar and Özen 2005).

Figure 5 compares the 5% damped elastic response spectra at Mae Sai station and Thai seismic design spectra, DPT 1302 (2009). By adopting model of ASCE 7-05 with some modification to engineering design coefficients to reflect real application for Thai buildings, the DPT 1302 code requires the SA values at 0.2 and 1.0 s with 2 percent of probability of exceedance in 50 years for defining Maximum Considered Earthquake (MCE) ground motion. These SA values have been obtained by a series of seismic hazard maps developed by Ornthammarath et al. (2011) and Palasri and Ruangrassamee (2010) with equal weights.

The recorded ground motions have been rotated to fault-normal and fault-parallel directions. The PGA of DPT 1302 spectra are 0.28 and 0.42 g for design and maximum considered earthquake levels, corresponding to 10 and 2 % probability of exceedance in 50 years, respectively. The observed spectral ordinates are less than that of design earthquake level, but it does exceed at 0.1 second. Both fault-normal and fault parallel components are comparable without any amplification at long period suggesting that there is no fault rupture directivity effect at Mae Sai station in agreement with observed damage. For strong motion of the largest aftershock, Mw 5.7 at 30 km distance, the PGA in NS, EW, and UD are 0.10, 0.07, and 0.04 g, respectively.

4.1 Seismological aspect of Mae Sai strong ground motion record

The acceleration records at Mae Sai station are shown in Figure 6 with the integrated velocity and displacement traces. Since there is a long pre-event motion to compute the pre-event mean with confidence, the lack of any drifts of the pre-event zero line in the velocity and displacement traces indicates that the baseline is stable in the pre-event portion of the record. However, this is not the case later during the shaking motion, the integrated raw velocity time series show a linearly trend that translate to a quadratic trend in the displacement traces. Thus a baseline correction is required to obtain more reliable results.

Even before baseline correction, the ramp in velocity and displacement time histories from 2 to 6 seconds on the NS component could be clearly identified. At first the ramp in velocity and displacement time histories were thought as artifacts due to unstable acceleration baselines; however, after considering a number of methods of baseline correction, the ramp are still observed and could be explained due to near- and intermediate-field terms in the elastic wave motion. In general, forward directivity and permanent translation are the two main causes for the one-side velocity pulses observed in near-field regions (Abrahamson 2000), even though other conditions (e.g., surface P-wave; Kawase and Aki 1990), supershear rupture velocity (e.g., Bouchon et al. 2001), or special geometrical conditions (e.g., Oglesby and Archuleta 1997) may also give rise or further intensify velocity pulses (Mavroeidis and Papageorgiou 2003).

For forward directivity, it occurs when the fault rupture propagates toward a site with a rupture velocity approximately equal to the shear-wave velocity. On the other hand, permanent translation at a site is a consequence of permanent fault displacement due to an earthquake. The displacement is not instantaneous but occurs over some finite duration of rupture resulting in step displacement and one-sided velocity pulse in the strike-parallel direction for strike-slip faults. Based on comparison of spectral acceleration in Fig. 5 and possible northeastward rupture direction on Sect. 2, the NS component of Mae Sai strong motion is more likely to display co-seismic ground displacement caused by the mainshock.

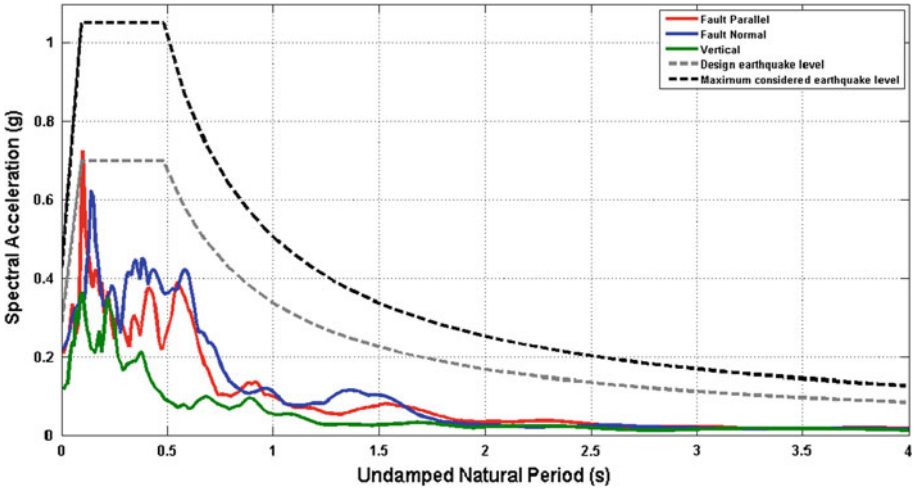

Fig. 5 Comparison of recorded spectral acceleration spectra (at 5 % damping) with Thailand seismic design spectra of soil type D for horizontal component at 10 and 2 % of exceedance in 50 years

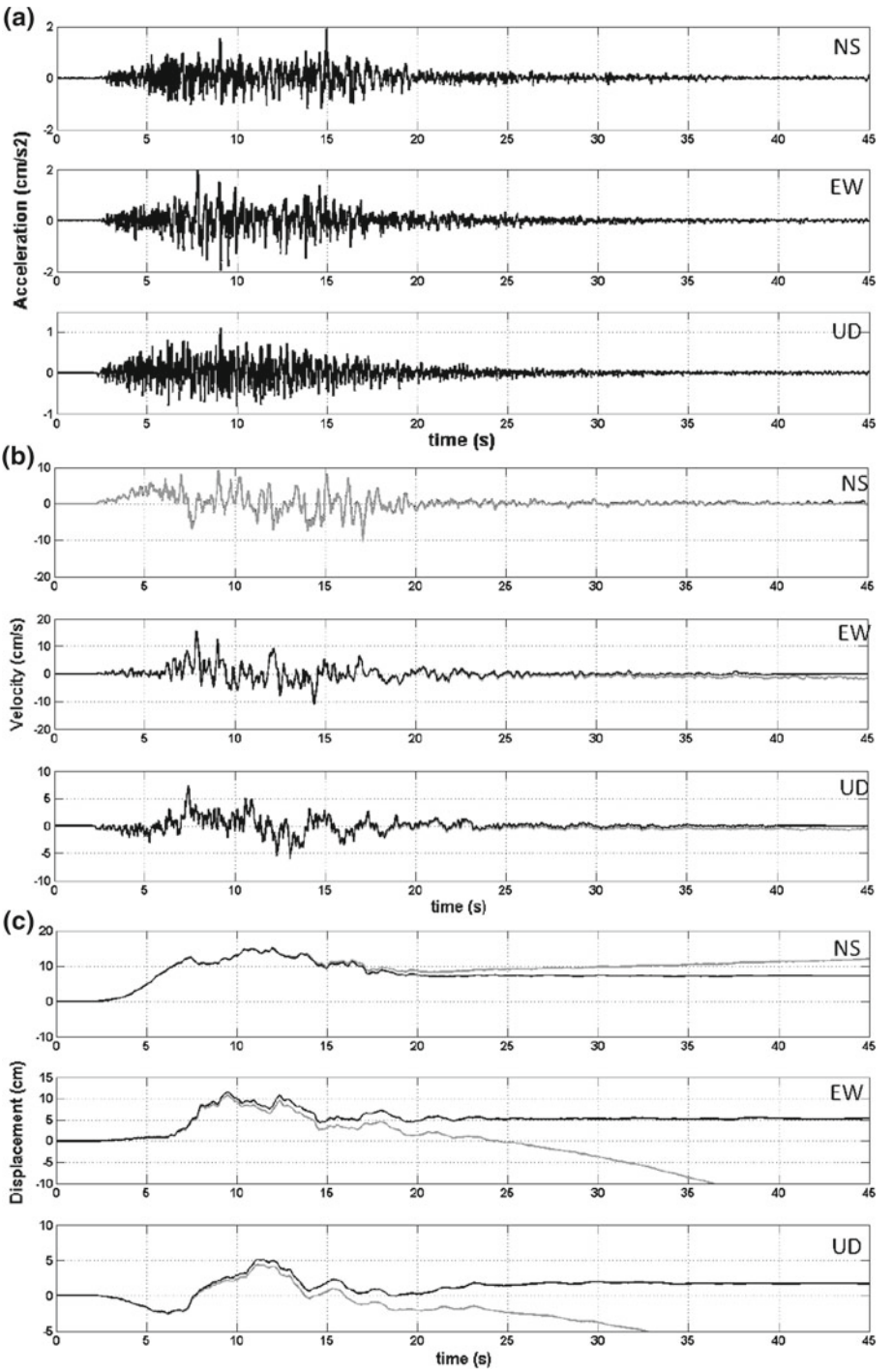

Fig. 6 **a** Acceleration, **b** velocity, and **c** displacement time histories for NS, EW, UD components with *gray lines* indicating raw data and *black lines* representing corrected data

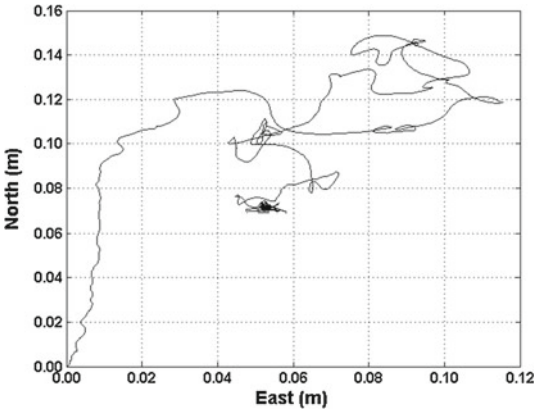

Fig. 7 Projection of particle motion on the north and east planes at Mae Sai station

By using baseline correction technique of Rupakhety et al. (2010), corrected velocity and displacement waveforms are displayed in Fig. 6 for three components. Black lines represent corrected velocities and displacement and grey lines correspond to velocities and displacement obtained by integrating raw acceleration. No digital filtering is performed on this acceleration time series. This is because high-pass filtering may remove low-frequency components of the signal carrying information pertaining to permanent displacement.

Both displacement waveforms obtained after baseline adjustment indicate permanent ground displacement toward the end of the record around 7, 5, and 1 cm for NS, EW, UD components, respectively. The analysis reveals that the ground has moved toward north-east as a results of the mainshock in agreement with style of faulting, Fig. 2. The particle motion projected on the horizontal plane is displayed in Fig. 7. The displacement show that at Mae Sai station exhibit initial northeastward movement followed by eastward movement before returning back. At the end of this event, this station is displaced toward north-east for 8 cm.

To testify the previous findings, the static displacement has been computed by using Coulomb 3.3 (Toda and Stein 2002; Lin and Stein 2004). Calculations are made in an elastic halfspace with uniform isotropic elastic properties following Okada (1992). The shear modulus of 3.2×10^{11} dyne-cm^{-2} and a uniform fault friction of 0.4 have been chosen. Because lower friction might be appropriate on the strike-slip faults (Parsons et al. 1999; Toda and Stein 2002), a friction coefficient of 0.0 has also been used which the results are little changed. In the Coulomb calculation, a 40 by 15 km rupture area with a 1.2 m uniform slip is assumed as the Coulomb source fault based on the Wells and Coppersmith (1994) relationship with focal mechanism and centroid location as provided by Global CMT solution, Tables 1 and 2.

From Fig. 8, the modeled displacement has been overlaid on Google Earth map showing that large displacement could be expected around near fault region. The modeled near field displacement are varied from 0.3 to 0.5 m in agreement with observation from field investigation. Furthermore, at Mae Sai station, the modeled static displacements are around 6, 3, and 1 cm for NS, EW, and UD direction, respectively. The comparison between modeled static displacement and those recovered from strong motion record are well consistent.

5 Conclusion

Based on available seismotectonic information and instrumental data, a summary of the 24 March 2011 Mw 6.8 Tarlay earthquake has been presented. The earthquake occurred along

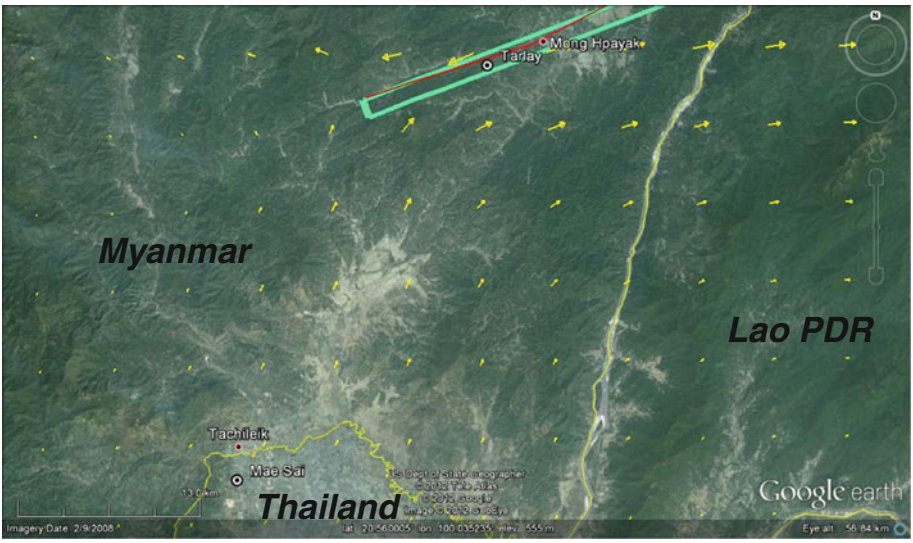

Fig. 8 Modeled static horizontal displacement on surface in *yellow arrows* is overlaid on Google Earth around western section of Nam Ma fault responsible for Mw 6.8, 24 March 2011 earthquake. The *red line* represents Nam Ma fault based on Lacassin et al. (1998), and the *green box* shows the modeled rupture zone of Tarlay earthquake

the western section of Nam Ma fault, which has been previously identified as an active fault; however, this secondary fault has been less studied than those two major active faults in this region (i.e. Sagaing and Red River faults). Observed strong ground motion has been compared with that of global empirical equations, and they are in fair agreement over the distance range for which the model is applicable. On the other hand, at long distance, the large positive and negative residuals suggest that a change in slope in the attenuation is not reflected in these GMPEs. Nevertheless, this should be expected since most GMPEs are derived to estimate ground motions up to 200 km. The observed 0.20 g PGA at Mae Sai station is currently the largest recorded PGA in Thailand; however, the observed spectra is lower than that provided in current Thailand seismic design code. This is in agreement with relatively less observed damage comparing to that inside Myanmar. Lastly, seismological aspect of observed strong motion at Mae Sai station has been further explained and compared with modeled static displacement which is in reasonable agreement.

Acknowledgments The information of strong ground motion data and related information provided by Seismological Bureau, Thai Meteorological Department (TMD) is highly appreciated. The author would like to extend his gratitude to local authorities for their supports during field survey. Thai earthquake reconnaissance team had been organized and supported by Chulalongkorn university. Moreover, the author would like to acknowledge Soe Thura Tun, Myanmar Earthquake Committee, and Dr. Yin Myo Min Htwe, Department of Meteorology and Hydrology, for a lot of fruitful discussion regarding earthquake damage inside Myanmar. Lastly, the author is grateful to an anonymous reviewer for his constructive comments that enhanced the quality of the paper.

References

Abrahamson NA (2000) Near-fault ground motions from the 1999 Chi-Chi earthquake. In: Proceedings of U.S.–Japan workshop on the effects of near-field earthquake shaking. San Francisco, California, 20–21 March 2000

Akkar S, Özen Ö (2005) Effect of peak ground velocity on deformation demands for SDOF systems. Earthq Eng Struct Dyn 34(13):1551–1571
AIT (1980) Asian Institute of Technology, "Investigation of Land Subsidence Caused by Deep Well Pumping in the Bangkok Area, Phase II". AIT research report submitted to the National Environmental Board, Thailand
Bilham R (2004) Earthquakes in India and the Himalaya: tectonics, geodesy and history. Ann Geophys 47(2):839–858
Boore DM, Atkinson GM (2008) Ground-motion prediction equations for the average horizontal component of PGA, PGV, and 5%-damped PSA at spectral periods between 0.01 s and 10.0 s. Earthq Spectra 24:99–138
Bouchon M, Bouin M-P, Karabulut H, Toksoz MN, Dietrich M, Rosakis AJ (2001) How fast is rupture during an earthquake? New insights from the 1999 Turkey earthquakes. Geophys Res Lett 28:2723–2726
DPT 1302 (2009) Seismic resistant design of buildings and structures. Department of Public Works and Town & Country Planning, Ministry of Interior, p 125 (in Thai)
Fenton CH, Charusiri P, Wood SH (2003) Recent paleoseismic investigations in northern and western Thailand. Ann Geophys 46:957–981
Giardini D, Grunthal G, Shedlock K, Zheng P (1999) The GSHAP global seismic hazard map. Annali di Geofisica 42:1225–1230
Kagawa T, Irikura K, Somerville PG (2004) Differences in ground motion and fault rupture process between the surface and buried rupture earthquakes. Earth Planets Space 56:3–14
Kawase H, Aki K (1990) Topography effect at the critical SV-wave incidence: possible explanation of damage pattern by the Whittier Narrows, California, earthquake of 1 October 1987. Bull Seismol Soc Am 80:1–22
Knopoff L (1958) Energy release in earthquakes. Geophys J 1:44–52
Lacassin R, Replumaz A, Hervé Leloup P (1998) Hairpin river loops and slip-sense inversion on southeast. Asian Strike Slip Faults Geol 26(8):703–706
Lin J, Stein RS (2004) Stress triggering in thrust and subduction earthquakes, and stress interaction between the southern San Andreas and nearby thrust and strike-slip faults. J Geophys Res 109:B02303. doi:10.1029/2003JB002607
Mavroeidis GP, Papageorgiou AS (2003) A mathematical representation of near-fault ground motions. Bull Seismol Soc Am 93(3):1099–1131
Oglesby DD, Archuleta RJ (1997) A faulting model for the 1992 Petrolia earthquake: can extreme ground acceleration be a source effect?. J Geophys Res 102:11877–11897
Okada Y (1992) Internal deformation due to shear and tensile faults in a half-space. Bull Seismol Soc Am 82(2):1018–1040
Ornthammarath T, Warnitchai P, Worakanchana K, Zaman S, Sigbjörnsson R, Lai CG (2011) Probabilistic seismic hazard assessment for Thailand. Bull Earthquake Eng 9(2):367–394
Palasri C, Ruangrassamee A (2010) Probabilistic seismic hazard maps of Thailand. J Earthq Tsunami 4(4):369–386
Parsons T, Stein RS, Simpson RW, Reasenberg PA (1999) Stress sensitivity of fault seismicity; a comparison between limited-offset oblique and major strike-slip faults. J Geophys Res 104(B9):20183–20202
Poovarodom N, Pitakwong K (2010) Microtremor observations for site characterization in Thailand. In: Proceeding of the 3rd Asia conference on earthquake engineering (ACEE2010):1–3 December 2010
Radiguet M, Cotton F, Manighetti I, Campillo M, Douglas J (2009) Dependency of near-field ground motions on the structural maturity of the ruptured faults. Bull Seismol Soc Am 2572–2581. doi:10.1785/0120080340
Ruangrassamee A, Ornthammarath T, Lukkunaprasit P (2012) Damage due to 24 March 2011 M6.8 Tarlay earthquake in Northern Thailand. In: Proceeding of the 15th world conference in earthquake engineering (15WCEE):Lisbon, Portugal, September 24–28, 2012
Rupakhety R, Halldorsson B, Sigbjornsson R (2010) Estimating coseismic deformations from near source strong motion records: methods and case studies. Bull Earthquake Eng 8(4):787–811. doi:10.1007/s10518-009-9167-9
Sadigh K, Chang C-Y, Egan JA, Makdisi FI, Youngs RR (1997) Attenuation relationships for shallow crustal earthquakes based on California strong motion data. Seismol Res Lett 68(1):180–189
Shen Z-K, Lu J, Wang M, Burgmann RC (2005) Contemporary crustal deformation around the southeast borderland of the Tibetan Plateau. J Geophys Res 110:B11409. doi:10.1029/2004JB003421
Sigurdsson SU, Rupakhety R, Sigbjornsson R (2011) Adjustments for baseline shifts in far-fault strong-motion data: an alternative scheme to high-pass filtering. Soil Dyn Earthq Eng 31(12):1703–1710
Stein S, Wysession M (2003) An introduction to seismology, earthquakes, and earth structure. Blackwell, ISBN 0-86542-078-5
Toda S, Stein RS (2002) Response of the San Andreas fault to the 1983 Coalinga-Nuñez earthquakes: an application of interaction-based probabilities for Parkfield. J Geophys Res 107. doi:10.1029/2001JB000172

Uttamo W, Elders CF, Nicols GJ (2003) Relationships between Cenozoic strike-slip faulting and basin opening in northern Thailand, in Intraplate Strike-Slip Deformation Belts, edited by F. Storti et al. Geol Soc Spec Publ 210:89–108

Wald DJ, Quitoriano V, Heaton TH, Kanamori H (1999) Relationships between peak ground acceleration, peak ground velocity, and Modified Mercalli intensity in California. Earthq Spectra 15(3):557–564

Wells DL, Coppersmith KJ (1994) New empirical relationships among magnitude, rupture length, rupture-width, and surface displacements. Bull Seismol Soc Am 84(4):974–1002

Worden CB, Gerstenberger MC, Rhoades DA, Wald DJ (2012) Probabilistic relationships between ground-motion parameters and modified mercalli intensity in California. Bull Seismol Soc Am 102(1):204–221